Evaluation and Correction of Angular Anisotropic Effects in Multidate SPOT and Thematic Mapper Data

Etienne Muller

Centre d'Ecologie des Resources Renouvelables, Toulouse, France

SPOT XS oblique data are compared with Landsat Thematic Mapper (TM) vertical data at two different times. Under the assumption that analogous spectral bands are equivalent, the differences in spectral responses observed over land cover classes are attributed to the effects of angular anisotropic reflection. This article shows that land cover classes cannot easily be characterized by their anisotropy. The magnitude of anisotropy varies strongly with the radiometric processing levels (i.e., absolute calibration or normalization) but has no significant impact on the overall classification results. The normalization method based on the use of pseudoinvariant objects is sufficiently effective as to correct most anisotropic disturbances and should facilitate an alternative use of SPOT and TM data.

INTRODUCTION

It is generally assumed that ground objects can be identified and characterized by specific spectral signatures. These signatures, however, are not only dependent upon intrinsic features of the objects but of many other factors such as sensor characteristics, sun–target–satellite geometry, date of acquisition, atmospheric parameters, and local environment. As a consequence, many difficulties arise in obtaining reliable biunivocal relationships between satellite data and physical ground parameters.

The usual approach consists in an absolute calibration of data (Markham and Barker, 1986; Slater et al., 1987; Begni, 1988; Hill and Aifadopoulou, 1990; Moran et al., 1992; Santer et al., 1991). Digital counts of images are converted into at-satellite (i.e., "apparent" or "top-of-atmosphere") radiance or reflectance and the atmospheric disturbances are removed from the signal. In the process, some approximations have to be made, and the signal correction is only partly successful, especially when calibration coefficients are not accurately known or when input parameters for the atmospheric correction models are estimated but not measured.

A second approach consists in the correction of data using image-based parameters only. Several methods have been described in the literature such as the dark-object subtraction technique (Chavez, 1988; 1989), the radiometric normalization method using pseudoinvariant objects (Schott et al., 1988), or the radiometric rectification based on the darkest and brightest values in images (Hall et al., 1991). These methods can be considered as relative calibration methods.

In both approaches, problems exist when spectral changes are analyzed with different sen-

Address correspondence to Etienne Muller, CERR / CNRS, 29 rue Jeanne Marvig, 31055 Toulouse Cedex, France.

sors or at different view angles. The effects of sensor and angular anisotropic factors on the spectral signatures of ground objects cannot be quantified accurately unless images are acquired simultaneously. This cannot be achieved in practice with actual satellite data. *In situ* ground and atmospheric measurements are also necessary, but there is no meterological network for the acquisition of atmospheric parameters that could be integrated in correction models.

Differences between sensors and between view angles can be partly evaluated if some compromises are accepted. In this paper the three SPOT bands (i.e., XS1, XS2, XS3) were compared with the equivalent TM bands (i.e., TM2, TM3, TM4) using "simultaneously" acquired images (i.e., either the same day or within a 2-day period) on two different times in 1987. The sensor factor (SPOT vs. TM) could not be dissociated from the angular anisotropic factor (oblique vs. vertical) because SPOT data were oblique on both dates. However, this "system anisotropy" OBLIQUE*SPOT vs. VERTICAL*TM corresponds to the most likely alternative encountered either with archived data or with newly acquired images. It also emphasizes the need for accurate and robust corrections methods for multidate–multisensor–multiview images. In the perspective of an alternative use of SPOT and TM images, it is also important to know whether the differences which exist in data can be utilized, corrected, or simply ignored and if the radiometric corrections of data have a strong impact on the results.

REVIEW

Many authors have observed asymmetric diffuse scattering (i.e., non-Lambertian) properties for objects using either ground measurements (Staenz et al., 1981; Methy et al., 1981; Duggin and Philipson, 1982; Slater and Jackson, 1981; Gross et al., 1988), aerial photographs (Egbert and Ulaby, 1972), airborne scanners (Ott et al., 1981; D'Arodes et al., 1984; Royer et al., 1985), or satellite sensors (Cavayas, 1987; Le Men, 1987; Moran et al., 1990).

They developed the concepts of angular reflectivity (Egbert and Ulaby, 1972), angular anisotropy of reflectivity (Kriebel, 1976), directional reflectance (Ott et al., 1981), stereoradiometry (Guyot, 1983), directional factor function (Royer et al., 1985), or angular reflectance signature (Gerstl, 1988). All these concepts are similar in that they illustrate the fact that the intrinsic spectral response of ground objects is not a static parameter that can be analyzed without taking into account "disturbing" factors. Multiple interactions exist and the disturbing factors must be considered as part of the response. As a consequence, it remains difficult to appreciate separately the exact contribution of each individual factor (Colwell, 1974; Kimes et al., 1980; Gross et al., 1988).

The effects of off-nadir viewing as summarized by Royer et al. (1985) vary greatly with the wavelength and with the type of ground surface. In general, they are more pronounced when the plane of detection or the scanning plane is close to the plane of illumination, (e.g., with SPOT and TM). The effects are asymmetric about the nadir and accentuated with high solar zenith angles. Off-nadir viewing can significantly increase the radiance. The increase is higher when the sun is behind the sensor (i.e., down sun viewing) and the backscatter is then maximum (hot spot effect). When looking toward the sun (i.e., up sun), there are shadow effects due to vertical protrusions and the increase is less; in some cases, a decrease of radiance is observed.

Some models have been proposed to relate reflectances or radiances to viewing incidence angles, sun incidence angles, and azimuth angles. Smith et al. (1980) use the Minnaert empirical equations with sun and view incidence angles. Staenz et al. (1981) consider the view incidence angle only and obtain quadratic fits with crops and a linear fit with soil reflectances. Le Men (1987) proposes a theoretical model including the three types of view angles while Milton and Rollin (1988) use a graphic device to visualize the anisotropy of a shrub canopy as a function of wavelength and relative azimuth. However, good correlations between view or sun angles, and spectral data do not mean that these models can be used as predictors for automatic data interpretation or for extrapolation.

Angular anisotropy is often considered therefore as a disturbing effect which must be corrected. Royer et al. (1985) tested four empirical correction procedures based on data normalization using a mean radiance variation factor related

to viewing angles (i.e., pixel positions). Significant gains in classification were observed after correction of data. Singh and Cracknell (1986) suggested the correction of SPOT data using the nonsymmetric parabolic variation of radiances observed in AVHRR images as a function of view angles within the scan range of $\pm 56°$. Moran et al. (1990) obtained good overall view angle corrections on SPOT data using ground-based bidirectional measurements acquired on satellite overpass days.

It has also been suggested that angular anisotropy may be an additional potential tool to improve the discrimination of ground objects. But this potential method has not yet been evaluated comprehensively with SPOT data or integrated in routine investigations. The basic reason is that an experimental approach is not easy to implement with satellite data for the development of anisotropic models. Simultaneous acquisitions of oblique and vertical images are not strictly possible over the same area.

Accurate radiometric and atmospheric corrections are also required for data comparison. The efficiency of the absolute calibration approach depends upon the availability of updated calibration coefficients and upon atmospheric parameters and models. After some initial alteration during the satellite's launch, TM calibration has been remarkably stable. Five ground verifications in White Sands, New Mexico over a 16-month period showed only a $\pm 2.8\%$ standard deviation from the mean, for all dates and all six reflective bands (Slater et al., 1987). The uncertainty on TM absolute calibrations were probably less than $\pm 5\%$ (Holm et al., 1989). The good stability of TM calibration throughout the period from 1984 to 1988 was confirmed by Hill and Aifadopoulou (1990). For SPOT data, three ground calibration campaigns were undertaken in La Crau, France, in 1989, and a detailed error budget showed that the error on calibration coefficients were ranging from 2.0% to 3.2% on days with extremely good visibilities and from 4.4% to 6.3% on a day where the visibility was low (Santer et al., 1991). In two additional campaigns in 1989, the objective was the intercalibration of SPOT, TM, and AVHRR data (Gu et al., 1991). Results indicated that the global uncertainty on the intercalibration of SPOT and TM was close to $\pm 4.5\%$ in the visible bands and $\pm 3\%$ in the near infrared band.

The importance of the atmospheric correction model in the absolute calibration of data was stressed by Moran et al. (1992), who assessed the accuracy of several procedures by reference to aircraft-based measurements of surface reflectance. The best results were obtained with radiative transfer codes and on-site atmospheric measurements. The rms error was approximately 0.012 reflectance with no significant difference between the three RTC tested. Acceptable rms errors close to ± 0.02 reflectance were obtained using estimates of atmospheric conditions.

METHOD

Simultaneous SPOT XS and TM data (i.e., acquired either the same day or within a few-day period) were compared from over the Garonne river valley near Toulouse, France at two different times in 1987 (Table 1). The images were geometrically registered on a 10 m $\times$ 10 m grid using splin-cubic biconvolutions on a Multiscope image processing system. A 10-m reference grid was chosen because the analysis was undertaken with SPOT panchromatic data as well, but the results will not be presented here. The registration accu-

Table 1. Characteristics of SPOT XS and Landsat TM Images Used for the Study

	April Data		*July Data*	
	SPOT XS	*TM*	*SPOT XS*	*TM*
Satellite	SPOT1	Landsat 5	SPOT1	Landsat 5
Instrument	HRV1	TM	HRV2	TM
Acquisition date	25 April 1987	23 April 1987	5 July 1987	5 July 1987
View incidence angle	19.3°W	0°	29.6°E	0°
Acquisition time (U.T.)	10.46	10.05	11.21	10.01
Preprocessing level	1B	5	2A	5
Path-row	041-261	199-29	041-261	198-30

racies computed over 32 control points ranged from 0.65 pixels to 1.01 pixels with maximum deviations from 1.44 pixels to 2.55 pixels.

Raw Data

Geometric registration of images constitutes a preliminary step to the analysis in most multidate studies. In the process, data are slightly modified but can still be considered as "raw" data. All disturbing factors (i.e., view angles, sensor characteristics, sun illumination, and atmospheric conditions) are integrated in the signal. Raw data represent the less accurate mean to evaluate the anisotropy of ground objects or the between-sensor differences.

At-Satellite Radiance

Raw digital counts (DC) in each spectral band were converted into at-satellite radiances (L) using a linear transform with absolute calibration coefficients a_0 and a_1 [Eq. (1), Table 2a]. For TM data, the updated coefficients were the same than those used by Hill and Aifadopoulou (1991). For SPOT data, the coefficients were extracted from the tapes and adjusted for a better reliability by linear interpolation between two control dates in

Table 2. Parameters for Radiometric Corrections

		Green Band		*Red Band*		*Infrared Band*	
		SPOT	*TM*	*SPOT*	*TM*	*SPOT*	*TM*
(a) Absolute calibration coefficients							
April	a_1	1.166	1.385	1.261	1.102	1.054	0.885
	a_0	0.000	−2.346	0.000	−1.897	0.000	−1.942
July	a_1	1.174	1.385	1.130	1.102	1.016	0.885
	a_0	0.000	−2.346	0.000	−1.897	0.000	−1.942
(b) Sun illumination parameters							
April	Solar zenith angle	34.5	39.9	34.5	39.9	34.5	39.9
	Solar azimuth angle	149.8	135.2	149.8	135.2	149.8	135.2
	Exoatmospheric irradiance	1850	1829	1610	1557	1090	1047
	Sun–earth distance correction	1.0111	1.0100	1.0111	1.0100	1.0111	1.0100
July	Solar zenith angle	22.7	31.4	22.7	31.4	22.7	31.4
	Solar azimuth angle	155.9	121.1	155.9	121.1	155.9	121.1
	Exoatmospheric irradiance	1840	1829	1570	1557	1040	1047
	Sun–earth distance correction	1.0335	1.0337	1.0335	1.0337	1.0335	1.0337
(c) Atmospheric parameters							
April	Horizontal visibility	12	15	12	15	12	15
	Optical depth	0.466	0.388	0.355	0.301	0.242	0.208
	Gaseous transmission	0.925	0.908	0.929	0.934	0.968	0.960
	Atmospheric reflectance	0.070	0.053	0.045	0.035	0.024	0.019
	Spheric albedo	0.152	0.141	0.120	0.107	0.077	0.069
	Downward transmission	0.850	0.862	0.886	0.893	0.915	0.920
	Upward transmission	0.873	0.900	0.904	0.924	0.929	0.944
July	Horizontal visibility	12	8	12	8	12	8
	Optical depth	0.466	0.582	0.355	0.465	0.242	0.330
	Gaseous transmission	0.934	0.919	0.930	0.936	0.930	0.920
	Atmospheric reflectance	0.068	0.065	0.044	0.045	0.023	0.026
	Spheric albedo	0.159	0.175	0.120	0.141	0.077	0.097
	Downward transmission	0.870	0.827	0.901	0.860	0.927	0.891
	Upward transmission	0.860	0.858	0.894	0.887	0.921	0.912
(d) Normalization coefficients							
April	A_1	0.796	1.000	1.098	1.000	0.993	1.000
	A_0	−5.63	0.00	−5.76	0.00	−6.15	0.00
July	A_1	1.207	1.317	1.345	1.188	1.385	1.005
	A_0	−30.76	−21.23	−22.11	−15.54	−33.51	−15.73

1987, following the recommendations made by Begni (1988).

$$L_\lambda^* = a_0 + a_1 \cdot \mathrm{DC}_\lambda. \quad (1)$$

At-Satellite Reflectance

The differences in sun illumination between data (Table 2b) were compensated by transforming at-satellite radiances into at-satellite reflectances using

$$\rho_\lambda^* = \frac{\pi \cdot d^2 \cdot L_\lambda^*}{E_\lambda \cdot \cos \theta_s}. \quad (2)$$

Atmosphere-Corrected Reflectance

Atmospheric corrections were then applied using the "5 S" model developed by Tanré et al. (1986). In a comparison of SPOT and TM data, Hill and Aifadopoulou (1990) found that the "5 S" model produced good coincidence between satellite- and ground-measured reflectance factors. The model was also successfully tested by Moran et al. (1992) with estimated atmospheric parameters. In the present study, horizontal visibilities at airports were the only realtime observed parameters that could be injected in the "5 S" model. The study area was located at respectively 20 km and 40 km from the two closest airports where different horizontal visibilities were generally observed. As in most studies, atmospheric conditions could only be evaluated approximately. In April, a midlatitude winter model (U H2O = 0.853 g/cm^2; U O3 = 0.395 cm atm) was used. In July, a midlatitude summer model (U H2O = 2.93 g/cm^2; U O3 = 0.319 cm atm) was used. Continental aerosol were assumed on both dates. Atmospheric parameters were then computed with the "5 S" model (Table 2c) and used for data corrections in the following equation:

$$\rho_\lambda = \frac{\rho^* - t \cdot \rho_a}{s \cdot (\rho^* - t \cdot \rho_a) + t \cdot T\theta_v \cdot T\theta_s}. \quad (3)$$

Normalized Data

For comparison with the absolute calibration approach, raw data were normalized using image-based parameters. Several authors suggested an empirical method for data normalization based on the use of (pseudo)invariant objects (Hertzog and Sturm, 1975; Blanc et al., 1978; Royer et al., 1988; Schott et al., 1988; Chavez, 1988; Hall et al., 1991). Large urban zones are sometimes chosen as radiometrically invariant objects. In this study a set of 19 pseudoinvariant objects was selected and considered as lambertian and radiometrically stable in time (i.e., water reservoirs, large buildings, gravel pits, and dense old pine plantations). When these objects are observed individually, the radiometric invariance is not strictly verified; but it was assumed that the mean radiometric value and the standard deviation of the entire set of pseudoinvariant objects remained invariant in each spectral band. The April TM image had the best radiometric range and was taken as radiometric reference (Table 2d). Other images were normalized by reference to it, according to Eq. (4). The method differs from that of Hall et al. (1991) in the choice of radiometric references. Hall et al. (1991) transformed data into Kauth–Thomas greenness and brightness indices and selected the dark and bright nonvegetated extremes in the two-dimension diagram. Control sets did not necessarily correspond to the same pixels from image

Table 3. Hierarchical Landcover Classification Scheme[a]

6 Classes	*10 Classes*	*20 Classes*	*27 Classes*
Urban	Urban	1 Village	Village
		2 Building	Building
Agriculture	Winter crops	3 Wheat	Wheat
		4 Barley	Barley
		5 Pea	Pea
	Spring crops	6 Rape	Rape
		7 Maize	Maize
		8 Sunflower	Sunflower
	Permanent crops	9 Orchard	Orchard
		10 Vineyard	Vineyard
Scrub	Scrub	11 Scrub	Scrub
Forest	Deciduous forest	12 Riparian wood	Riparian wood
		13 Poplar	Young poplar
			Mature poplar
			Old poplar
		14 Oak	Young oak
			Mature oak
		15 Hornbeam	Hornbeam
	Evergreen forest	16 Evergreen forest	Young pine
			Mature pine
			Old pine
	Mixed forest	17 Mixed forest	Mixed forest
Water	Water	18 Water	Stream
			Pond
			Reservoir
Barren land	Barren land	19 Clearcut	Clearcut
		20 Gravel pit	Gravel pit

[a] Class numbers are used in Figures 2, 3, and 4.

to image. In the present study, pseudoinvariant objects corresponded to fixed pixels in images:

$$NDC = A_0 + A_1 \cdot DC \quad (4)$$

with $A_1 = \sigma_0 / \sigma$ and $A_0 = \overline{DC_0} - \overline{DC} \cdot \sigma_0 / \sigma$, where $\overline{DC_0}$ and σ_0 are the mean value and the standard deviation of pseudoinvariant objects in the reference image and $\overline{DC}$ and σ are the mean value and the standard deviation of pseudoinvariant objects in the image to be corrected.

The Landcover Classes

After several ground investigations, 27 landcover classes were selected as being most representative of the study area. They were further grouped in a hierarchical scheme into 20, 10, and 6 higher ranked classes (Table 3). Five test sites were chosen for each of the 27 landcover classes. Over each test site one square training field of 7×7 pixels was extracted in the 10-m image database. Each training field was equivalent to ca. 0.5 ha. The undesirable effects related to differences in ground resolution (20 m and 30 m) and to the modification of data due to the geometric registration of images were reduced by the extraction of training fields from large homogeneous test sites. Problems of topographic effects were avoided by selecting the test sites on horizontal areas only.

RESULTS

Characterization of Anisotropic Effects

Mean Anisotropic Effects

The mean differences between oblique SPOT and vertical TM data were computed for each spectral band over the entire set of 27 landcover classes (Table 4a). The interpretation of the mean differences is not really possible with raw data as the results integrate all disturbing factors (i.e., view angles, sensor characteristics, illumination, and atmospheric conditions). After illumination and atmospheric corrections and assuming that the spectral sensitivities of the three SPOT bands were equivalent to the corresponding TM bands, the mean differences in data were attributed, as a first approximation, to angular anisotropic effects only. In April, with the sun behind the sensor, the west looking (−19.3°) SPOT oblique image had always higher reflectance values than the

Table 4. Comparison of SPOT and TM Data over 135 Test Sites (27 Landcover Classes), with Between-Site Standard Deviations (s.d.)[a]

		Green Band		*Red Band*		*Infrared Band*	
		Mean	*s.d.*	*Mean*	*s.d.*	*Mean*	*s.d.*
(a) Mean differences (SPOT − TM)							
April	Raw data	17.1	2.7	3.5	3.1	5.7	4.5
	At-satellite radiance	14.8	2.9	11.5	3.0	19.8	4.7
	At-satellite reflectance	0.0229	0.0070	0.0185	0.0085	0.0450	0.0137
	Atmosphere corrected reflectance	0.0107	0.0094	0.0150	0.0103	0.0493	0.0158
	Normalized data	1.0	2.2	1.3	2.7	−1.0	4.6
July	Raw data	10.9	1.8	−0.5	3.3	−9.6	6.8
	At-satellite radiance	6.3	2.8	2.5	3.5	3.2	4.2
	At-satellite reflectance	0.0027	0.0066	−0.0031	0.0101	−0.0072	0.0185
	Atmosphere corrected reflectance	−0.0069	0.0107	−0.0062	0.0148	−0.0210	0.0263
	Normalized data	−1.1	2.4	−0.9	3.0	0.9	4.0
(b) Mean ratios (SPOT / TM)							
April	Raw data	1.527	0.116	1.146	0.117	1.133	0.152
	At-satellite radiance	1.359	0.118	1.400	0.167	1.421	0.261
	At-satellite reflectance	1.252	0.109	1.262	0.151	1.272	0.233
	Atmosphere corrected reflectance	1.223	0.201	1.352	0.288	1.322	0.386
	Normalized data	1.039	0.061	1.054	0.082	1.002	0.075
July	Raw data	1.267	0.062	1.005	0.070	0.906	0.086
	At-satellite radiance	1.121	0.060	1.080	0.086	1.074	0.120
	At-satellite reflectance	1.031	0.055	0.991	0.079	1.000	0.112
	Atmosphere corrected reflectance	0.943	0.096	0.986	0.135	0.969	0.139
	Normalized data	0.976	0.062	0.990	0.081	1.007	0.066

[a] Raw and normalized data are in digital count (DC), radiance data are in W / m² μm sr, reflectance data are unitless.

TM vertical image (Table 4a). In July, with the east-looking (+29.6°) SPOT oblique image the differences in reflectance after atmospheric corrections were much lower than in April and always negative. The differences were in general similar in the green and red bands but three to five times higher in the near infrared band. With normalized data, the mean differences between oblique and vertical data were close to 1 DC in each spectral band, indicating a good overall fit of data.

Overall anisotropic effects were also evaluated by the ratios of oblique data divided by vertical data (Table 4b). Ratios provided information on the relative importance of anisotropic disturbances and could be easily transformed into percentages. They also permitted comparisons between the radiometric corrections methods. Results showed that with atmosphere-corrected reflectance the mean anisotropic effects varied from +22% to +35% in April and from −1% to −6% in July while the normalization of data produced good adjustments on both dates with anisotropic effects ranging from −2% to +5% only. However, as indicated by the between-sites standard deviations, all sites and all landcover classes were not affected to the same extent by anisotropic effects.

By-Class Anisotropic Effects

A visual comparison of the mean spectral values for each of the 135 test sites showed that radiometric calibration and normalization methods had different impacts on the quality of the overall adjustment of SPOT and TM data (Fig. 1). It also gave evidence that if the spectral sensitivities of SPOT and TM bands are not strictly the same, they can be considered as almost equivalent and be adjusted by simple translations (e.g., normalization method). However, after such transforms, differences between SPOT and TM data still persist in some landcover classes.

The best evaluation of by-class anisotropic effects is provided by atmosphere-corrected reflectances and can be computed by the absolute difference between data (Fig. 2). It can also be computed as a percentage of modification of the signal for comparison with normalized data (Figs. 3 and 4). Results confirmed less disturbances in the July east-looking image than in the April west-looking image. In April, the highest disturbances (hot spot effects) were observed for winter-planted crops and forests in the visible bands, and for water in the near-infrared band.

However, analysis of variances revealed an absence of interaction between the view angle factor and the landcover class factor in April. The between-class differences were never significant (Table 5). In July, the interactions were always significant with atmosphere-corrected reflectances but not with normalized data, indicating that the anisotropic effects could be reduced by the normalization of data but not by the absolute calibration of data.

Errors Analysis

When SPOT oblique images are used rather than TM images systematic disturbances or "bias" are introduced in spectral signatures. But these bias (i.e., the mean differences by spectral band) are not stable. They vary with time and affect differently the landcover classes. The best evaluation is obtained with the absolute calibration of data but uncertainties on sensor calibrations coefficients and on atmospheric parameters will always maintain substantial errors in the estimates. These errors cannot be computed and corrected unless atmospheric measurements and ground calibration controls are made systematically for each image acquisition. This is not feasible in routine investigation by normal users. In this study, errors were evaluated globally by the unexplained variance between oblique SPOT and vertical TM data and designated as residual error. The residual errors include differences in spectral sensitivities between SPOT and TM detectors and local variabilities within landcover classes once the contribution of the view angle factor and of the landcover class factor has been isolated in analysis of variance (Table 5). With normalized data, residual errors were close to 2–3 DC in the green band, 3 or 4 DC in the red band, and 6–8 DC in the infrared band. With atmosphere corrected reflectance, the errors ranged from 0.008 to 0.015 (excepted in April with 0.028 in the infrared band). These errors have the same magnitude than those observed between TM and aircraft data over bare soil and full-cover vegetation (Holm et al., 1989). The authors obtained rms errors ranging from 0.006 to 0.010 with atmospheric corrections and from 0.017 to 0.031 without atmospheric corrections. Over the same area but over

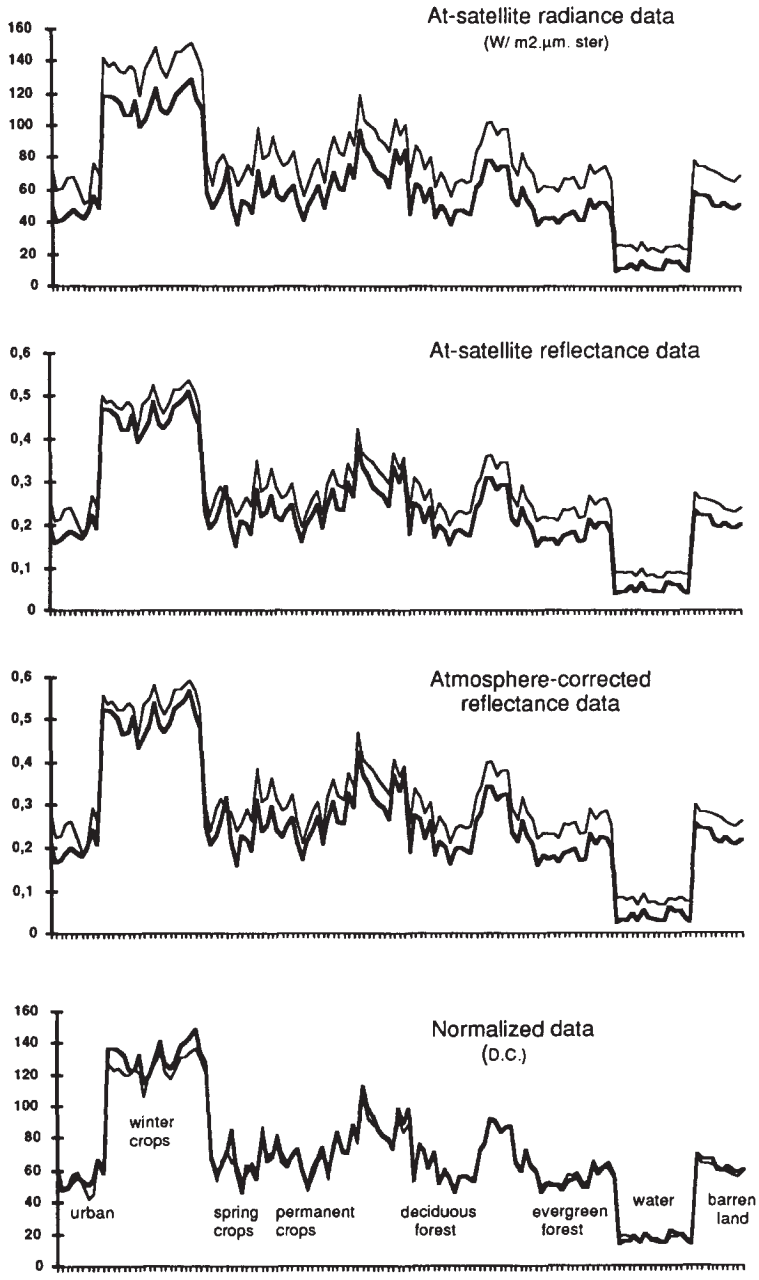

Figure 1. Comparison of SPOT and TM data over 135 test-sites in the infrared band in April: (—) SPOT; (–) TM.

a longer period of investigation, Moran et al. (1992) obtained RMS errors ranging from 0.012 to 0.020 depending on the radiative transfer codes and on the input parameters used.

Utilization of Anisotropic Effects

Although the interactions between the view angle and the landcover classes were not always statistically significant, it was important to control whether or not the anisotropic disturbances in data had an impact on classification results. The discrimination efficiency of individual spectral bands was first compared using F-tests (Table 6). Results showed that anisotropic differences or anisotropic ratios alone were considerably less efficient at distinguishing different landcover classes than the original bands, especially with April data. Only the infrared reflectance ratio in July produced a high F-value which was close to that of original bands. The absolute calibration or normalization of data consisting of linear or quasilinear transforms had no impact on the discrimination efficiency of original bands. But the

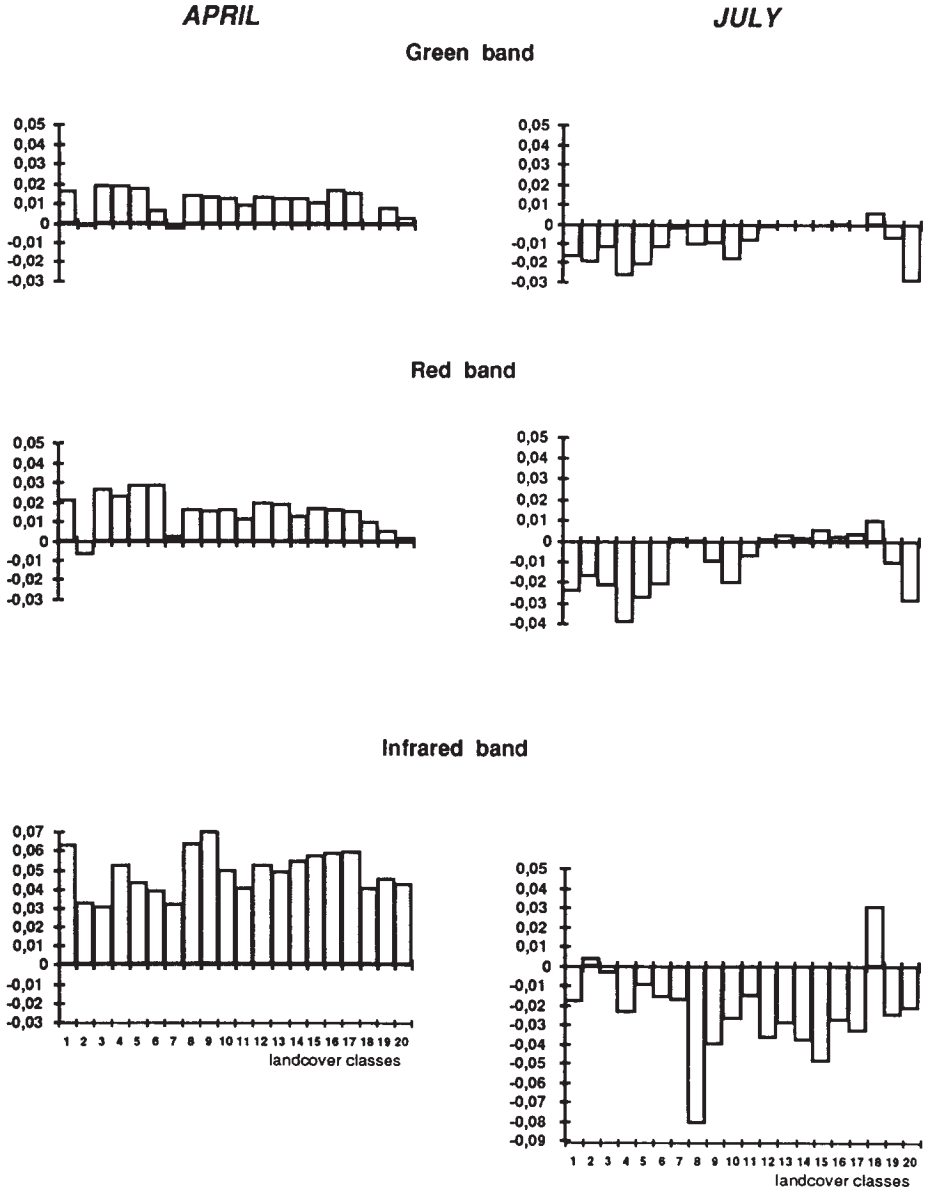

Figure 2. Evaluation of by-class anisotropic differences (SPOT – TM) for 20 landcover classes (in atmosphere-corrected reflectance).

normalization method produced substantial decreases of F-values in all bands with the anisotropic differences and ratios, while the absolute calibration of data generally maintained or increased F-values.

Several band combinations were also compared using a classification method based on discriminant analysis and Mahalanobis distances as described by Foucart (1982). Results confirmed that the anisotropy of objects as a single source of information (i.e., anisotropic differences or ratios) was not sufficient to correctly distinguish landcover classes (Table 7). The original bands were more efficient than anisotropic data alone and provided 10–33 additional points in the overall percentage of well-classified pixels. Combination of original spectral bands together with anisotopic differences provided modifications of the results ranging from -5 to $+8$ points. The classification results also showed that the radiometric corrections had almost no impact on the discrimination efficiency of images.

Additional tests were undertaken in order to see if there was any significant change in the results between different classification methods (i.e., discriminant analysis, maximum likelihood, and hypercubic methods). Three perception levels corresponding to 6, 10, and 20 landcover

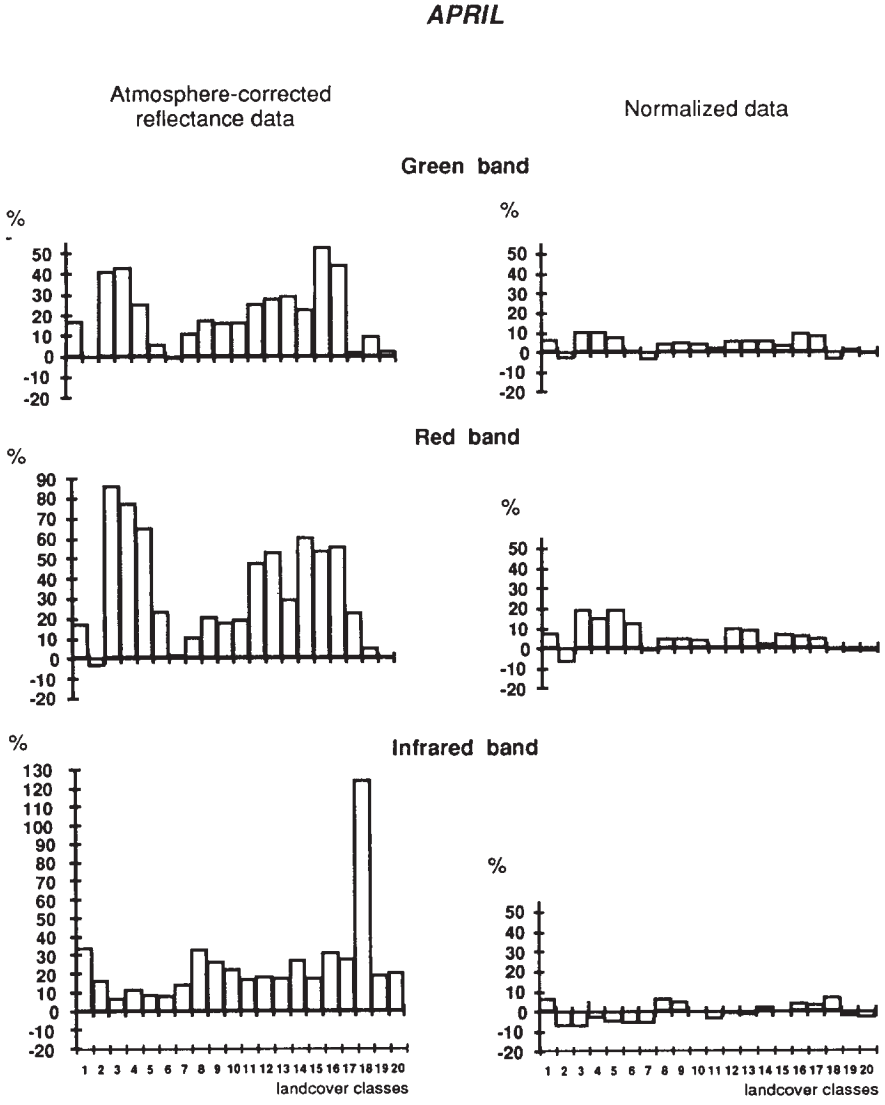

Figure 3. Evaluation of anisotropic effects for 20 landcover classes in April. The percentage of modification of the signal was computed as follows: % = 100 × (SPOT − TM) / TM.

classes were also compared (Table 8). An analysis of variance based on the by-class percentage of well-classified pixels did not show any significant differences between oblique and vertical data while the date of acquisition and the classification method were highly significant. This indicates that standard pixel by pixel classification methods currently available on conventional image processing systems cannot take advantage of the additional information provided by the anisotropy of objects in overall landcover mapping projects.

Correction of Anisotropic Effects

As no significant differences in classification results were observed between oblique SPOT and vertical TM images, there was no real need to correct anisotropic effects in data. However, if an absolute quantification of spectral changes through time is required (particularly in multisensor analysis), the accurate adjustment of data is necessary. As shown in Table 5, the correction of raw data into reflectance data always produced very highly significant anisotropic differences between SPOT and TM data (i.e., on both dates and in all spectral bands).

In contrast, the normalization method based on the use of fixed pseudoinvariant sites in images could correct the main disturbing factors. The overall bias between oblique and vertical data was reduced to about 1 DC (Table 4). They were highly significant in the visible bands but not significant anymore in the infrared band (Table 5). These levels of significance were confirmed by nonparametric Kruskal–Wallis rank tests. They indicate that the normalization method can re-

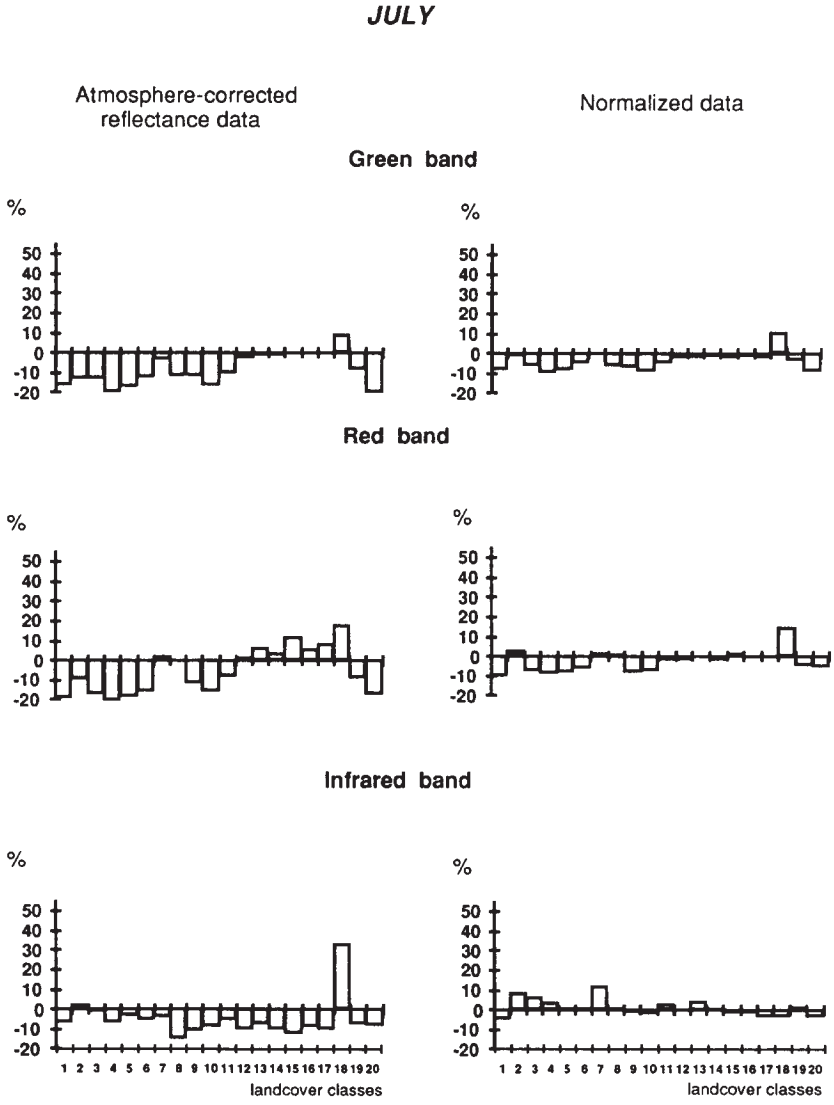

Figure 4. Evaluation of anisotropic effects for 20 landcover classes in July. The percentage of modification of the signal was computed as follows: % = 100 × (SPOT − TM) / TM.

Table 5. Analysis of Variance by Date and by Spectral Band for Atmosphere-Corrected Reflectance and Normalized Data[a]

Factors	Degrees of Freedom (Total = 269)	Green Band		Red Band		Infrared Band	
		Atm.-Corr. Reflectance	*Normalized Data*	*Atm.-Corr. Reflectance*	*Normalized Data*	*Atm.-Corr. Reflectance*	*Normalized Data*
April							
View angle	1	49.5***	8.2**	71.2***	6.9**	217.2***	1.6
Landcover	26	103.2***	02.7***	126.4***	25.8***	223.8***	22.6***
View*Landcover	26	0.8	0.7	0.8	0.7	0.4	0.8
Residual error	216	0.0125	2.9	0.0146	4.0	0.0275	6.6
July							
View angle	1	52.6***	10.6**	23.5***	3.5	43.6***	0.9
Landcover	26	96.8***	97.3***	135.1***	36.8***	110.6***	07.8***
View*Landcover	26	4.1***	1.5	4.3***	0.7	2.2**	0.4
Residual error	216	0.0078	2.6	0.0106	3.8	0.0106	7.6

[a] Two factors are analyzed: view angle (oblique vs. vertical) and landcover (27 classes). In the table, data are F-ratios with their respective degrees of freedom and levels of significance. Residual errors are in DC for normalized data and are unitless for reflectance data. * Significant ($P < 0.05$), ** highly significant ($P < 0.01$), and *** very highly significant ($P < 0.001$).

Table 6. Comparison of the Discrimination Efficiency of Individual Bands over 20 Landcover Classes Using F-Tests with the Same Degrees of Freedom (19 / 115)[a]

		Green Band	*Red Band*	*Infrared Band*
(a) Original raw bands				
April	SPOT	63.6	76.6	111.1
	TM	65.3	90.6	100.8
July	SPOT	54.4	88.6	64.7
	TM	63.8	93.7	76.2
(b) Band differences (SPOT – TM)				
April	Raw data	7.7	12.7	7.7
	At-satellite radiance	4.5	6.3	10.9
	At-satellite reflectance	6.9	10.2	4.1
	Atmosphere corrected reflectance	6.2	8.4	4.2
	Normalized data	5.8	7.0	7.7
July	Raw data	9.1	21.0	33.9
	At-satellite radiance	16.9	18.4	14.8
	At-satellite reflectance	22.9	27.8	24.3
	Atmosphere corrected reflectance	27.9	32.8	31.7
	Normalized data	12.2	9.9	5.5
(c) Band ratios (SPOT / TM)				
April	Raw data	17.8	18.1	17.8
	At-satellite radiance	21.0	21.4	24.1
	At-satellite reflectance	21.0	21.4	24.1
	Atmosphere corrected reflectance	15.5	14.3	19.2
	Normalized data	9.3	8.8	3.6
July	Raw data	23.2	22.7	44.8
	At-satellite radiance	25.7	26.9	59.2
	At-satellite reflectance	25.7	26.9	59.3
	Atmosphere corrected reflectance	20.9	23.1	74.0
	Normalized data	14.7	12.4	3.0

[a] Radiometric corrections did not modify F-values of original raw bands.

duce considerably the overall anisotropic effects (including intersensor differences) but does not suppress them totally. The overall fit of data is better with the normalization method than with the absolute calibration of data (Fig. 1).

The normalization method is also capable to suppress the level of significance of between-class anisotropic effects when it exists (Table 5b). It is easy to use and does not modify significantly the classification results when compared with raw or

Table 7. Comparison of the Discrimination Efficiency of Images over 20 Landcover Classes Using Discriminant Analysis (in % of Well-Classified Test Sites)[a]

Date	*Processing Level of Data*	*Oblique Images*	*Vertical Images*	*Anisotropic Ratios (Oblique / Vertical)*	*Anisotropic Differences (Oblique – Vertical)*	*Vertical Images and Anisotropic Differences*
April	Raw data	69.6	71.1	50.4	52.6	65.9
	Atm.-corr. reflectance	70.4	72.6	51.9	38.5	65.9
	Normalized data	69.6	71.1	36.3	42.2	65.9
July	Raw data	55.6	58.5	43.7	45.2	60.0
	Atm.-corr. reflectance	56.3	59.3	40.0	51.1	60.0
	Normalized data	55.6	58.5	33.3	44.4	60.0
April + July	Raw data	75.6	76.3	69.6	65.9	82.2
	Atm.-corr. reflectance	75.6	76.3	65.2	63.7	83.0
	Normalized data	75.6	76.3	55.6	62.2	82.2

[a] The discriminant analysis refers to a classification method based on the computation of new axis and Mahalanobis distances as described by Foucart (1982).

Table 8. Comparison of the Discrimination Efficiency of Oblique and Vertical Raw Data Using Three Classification Methods over Hierarchical Landcover Classes (in % of Well-Classified Pixels)[a]

	Discriminant Analysis		*Maximum Likelihood*		*Hypercubic Method*	
Date	*Oblique*	*Vertical*	*Oblique*	*Vertical*	*Oblique*	*Vertical*
20 landcover classes						
April	69.6	71.1	68.6	66.2	73.2	72.0
July	55.6	58.5	63.5	61.2	69.8	64.9
April + July	75.6	76.3	82.5	84.6	89.7	88.4
10 landcover classes						
April	71.1	70.4	78.1	73.2	78.0	76.9
July	65.2	64.4	68.1	69.2	73.5	70.9
April + July	72.6	77.0	86.4	83.9	88.4	88.8
6 landcover classes						
April	67.4	68.9	81.4	73.6	83.5	82.7
July	66.7	69.6	72.0	72.6	80.9	77.9
April + July	71.9	74.8	88.4	85.1	91.8	91.7

[a] The Maximum Likelihood Method was used under the assumption of normality without *a priori* knowledge of by-class probability. The Hypercubic Method utilizes fuzzy logic for the characterization of classes by histograms. Both methods are described in the users' manual of the Multiscope image processing system.

reflectance data (Table 7). The method seems therefore promising for multisensor SPOT and TM image analysis. By extension, the same method is expected to be efficient in multidate studies for understanding spectral changes over a given area. Additional researches should improve the quality of data normalization (particularly in the selection procedure of pseudoinvariant objects) and should evaluate the accuracy of interregional spectral comparisons.

CONCLUSION

Radiometric comparisons of actual oblique-SPOT and vertical-TM images showed that differences existed between analogous spectral data and that the magnitude of these differences depended upon several factors. Four of these factors were examined: 1) the spectral bands, 2) the dates of acquisition, 3) the landcover classes, and 4) the radiometric corrections. All factors and parameters were not totally controlled. For example, the view angle factor could not be dissociated from the sensor factor. The observed anisotropy was the result of the combined view-angle-sensor factors but corresponds to the most frequent situation encountered by SPOT and TM users. The absolute evaluation of anisotropic effects was also implicitly weighted by the landcover sampling method. Therefore, the results should be confirmed by other studies under different conditions before generalization.

The results of this work indicated that:

- The magnitude of the modifications of the signal introduced by changes in view angles cannot be evaluated in the absence of accurate absolute radiometric and atmospheric correction procedures. These corrections cannot be assumed by normal users in routine investigations. Therefore, uncertainties in parameters will always maintain important and unknown errors in the absolute estimates of angular anisotropic effects. Moreover, as satellite data (for cost and technical reasons) cannot be easily integrated in comprehensive controlled experiments, the characterization and modeling of landcover classes by angular anisotropic signatures based on space data is rather improbable in a near future.
- The anisotropic information contained in space data is normally not accessible to users who acquire only one single image (either oblique or vertical but not both of them). This additional information, when it is known, does not produce significant differences in landcover classification results and therefore does not justify the acquisition of multiview images.
- The anisotropic effects might rather be

considered as disturbing factors for the interpretation of data. Then the normalization method based on the use of fixed pseudoinvariant objects in images can be proposed to reduce significantly the anisotropy of landcover classes. It is easy to apply and should facilitate spectral change analysis in multidate–multisensor–multiview investigations.

REFERENCES

Begni, G. (1988), SPOT data absolute calibration: a synthesis, CNES Internal Paper CT / APP / TI / IS No 208, 10 Aug.

Blanc, G., Fontanel, A., Lallemand, C., and Wadsworth, A. (1978). Corrections radiometriques des enregistrements Landsat en vue d'une comparaison de chronoséquences, Photo Interpretation No 5, 5a:30–35.

Cavayas, F. (1987), Modelling and correction of topographic effect using multitemporal satellite images, *Can. J. Remote Sens.* 13:49–67.

Chavez, P. S., Jr. (1988), An improved dark-object subtraction technique for atmospheric scattering correction of multispectral data. *Remote Sens. Environ.* 24:459–479.

Chavez, P. S., Jr. (1989), Radiometric calibration of Landsat Thematic mapper multispectral images, *Photogramm. Eng. Remote Sens.* 55:1285–1294.

Colwell, J. E. (1974), Vegetation canopy reflectance, *Remote Sens. Environ.* 3:175–183.

D'Arodes, M. C., Podaire, A., and Saint, G. (1984), Analyses des effets directionnels sur la végétation et les sols, in *Signatures Spectrales d'Objets en Télédétection*, Bordeaux, 12–16 Sep. 1983, I.N.R.A., Versailles, pp. 159–170.

Duggin, M. J., and Philipson, W. R. (1982), Field measurement of reflectance: some major considerations, *Appl. Opt.* 21:2833–2840.

Egbert, D. E., and Ulaby, F. T. (1972), Effects of angles on reflectivity, *Photogramm. Eng. Remote Sens.* 38:556–564.

Foucart, T. (1982), Analyse factorielle, programmation sur micro-ordinateurs, Masson, Paris.

Gerstl, S. A. W. (1988), The angular reflectance signature of the canopy hot spot in the optical regime, in *Spectral Signatures of Objects in Remote Sensing, 4th International Colloquium*, ESA SP-287, ESTEC, Noordwijk, The Netherlands, pp. 129–132.

Gross, M. F., Hardiski, M. A., and Klemas, V. (1988), Effects of solar angle on reflectance from wetland vegetation, *Remote Sens. Environ.* 26:195–212.

Gu, X. F., Verbrugghe, M., and Guyot, G. (1991), Inter-étalonnage de Spot1-HRV, Landsat5-TM et Noaa11-AVHRR dans les domaines du visible et du proche infrarouge, in *Physical Measurements and Signatures in Remote Sensing, Proceedings 5th International Colloquium*, Courchevel, France, ESA SP-319, ESTEC, Noordwijk, The Netherlands, pp. 45–48.

Guyot, G. (1983), Variabilitée angulaire et spatiale des données spectrales dans le visible et le proche infrarouge, in *Signatures Spectrales d'Objets en Télédétection*, Bordeaux, 12–16 Sep. 1983, I.N.R.A., Versailles, pp. 27–44.

Hall, F. G., Strebel, D. E., Nickeson, J. E., and Goetz, S. J. (1991), Radiometric rectification: toward a common radiometric response among multidate, multisensor images, *Remote Sens. Environ.* 35:11–27.

Hertzog, J. H., and Sturm, B. (1975), Preprocessing algorithms for the use of radiometric corrections and texture / spatial features in automatic land use classification, in *Proc. 10th Symp. Remote Sens. Environ.*, ERIM, Ann Arbor, MI, pp. 705–714.

Hill, J., and Aifadopoulou, D. (1990), Comparative analysis of Landsat-5 TM and Spot HRV-1 data for use in multiple sensor approaches, *Remote Sens. Environ.* 34:55–70.

Hill, J., and Sturm, B. (1991), Radiometric correction of multitemporal Thematic Mapper data for use in agricultural land-cover classification and vegetation monitoring, *Int. J. Remote Sens.* 12:1471–1491.

Holm, R. G., Jackson, R. D., Yuan, B., Moran, M. S., Slater, P. N., and Biggar, S. F. (1989), Surface reflectance factor retrieval from Thematic Mapper data, *Remote Sens. Environ.* 27:47–57.

Kimes, D. S., Smith, J. A., and Ranson, K. J. (1980), Vegetation reflectance measurements as a function of solar zenith angle, *Photogramm. Eng. Remote Sens.* 46:1563–1572.

Kriebel, K. T. (1976), On the variability of the reflected radiation field due to differing distributions of irradiation, *Remote Sens. Environ.* 4:257–264.

Le Men, M. (1987), Etude de la stéréoradiometrie sur les images SPOT, in *Spot-1, Image Utilization, Assessment, Results*, CNES, Paris pp. 1297–1303.

Markham, B. L., and Barker, J. L. (1986), Landsat MSS and TM post-calibration dynamic ranges, exoatmospheric reflectances and at-satellite temperatures, EOSAT Landsat Technical Notes No. 1, Aug., pp. 3–8.

Methy, M., Lacaze, B., and Dauzat, J. (1981), Cinétiques journalière et saisonnière des facteurs spectraux de réflectance directionnelle d'une culture de soja, et implications pour l'utilisation des données du satellite SPOT, in *Signatures Spectrales d'Objets en Télédétection*, Avignon, 8–11 Sept., I.N.R.A., Versailles, pp. 591–599.

Milton, E. J., and Rollin, E. M. (1988), A simplified reflectance model for shrub canopies, *4th International Colloquium on Spectral Signatures*, Aussois, ESTEC, Noordwijk, The Netherlands, pp. 147–150.

Moran, M. S., Jackson, R. D., Hart, G.F., et al. (1990), Obtaining surface reflectance factors from atmospheric and view angle corrected SPOT-1 HRV data, *Remote Sens. Environ.* 32:203–214.

Moran, M. S., Jackson, R. D., Slater, P. N., and Teillet, P. M. (1992), Evaluation of simplified procedures for retrieval of

land surface reflectance factors from satellite sensor output, *Remote Sens. Environ.* 41:169–184.

Ott, W., Pfeiffer, B., and Quiel, F. (1981), Directional reflectance properties determined by analysis of airborne multispectral scanner data and atmospheric correction, in *Signatures Spectrales d'Objets en Télédétection*, Avignon, 8–11 Sept., I.N.R.A., Versailles, pp. 521–530.

Royer, A., Vincent, P., and Bonn, F. (1985), Evaluation and correction of viewing angles effects on satellite measurements of bidirectional reflectance, *Photogramm. Eng. Remote Sens.* 51:1899–1914.

Royer, A., Charbonneau, L., and Teillet, P. M. (1988), Interannual Landsat MSS reflectance variation in an urbanized temperate zone, *Remote Sens. Environ.* 24:423–466.

Santer, R., Deuzé, J. L., Devaux, C., et al. (1991), Spot calibration on the test site 'La Crau'(France), in *Physical Measurements and Signatures in Remote Sensing, Proceedings 5th International Colloquium*, Courchevel, France, ESA SP-319, ESTEC, Noordwijk, The Netherlands, pp. 77–80.

Schott, J. R., Salvaggio, C., and Volchok, W. J. (1988), Radiometric scene normalization using pseudoinvariant features, *Remote Sens. Environ.* 26:1–16.

Singh, S. M., and Cracknell, A. P. (1986), The estimation of atmospheric effects for SPOT using AVHRR channel-1 data, *Int. J. Remote Sens.* 7:361–377.

Slater, P. N., and Jackson, R. D. (1981), Transforming ground-measured reflectances to radiances measured by various space sensors through clear and turbid atmospheres, *Signatures Spectrales d'Objets en Télédétection*, Avignon, 8–11 Sept., I.N.R.A., Versailles, pp. 531–542.

Slater, P. N., Biggar, S. F., Holm, R. G., et al. (1987), Reflectance- and radiance-based methods for the in-flight absolute calibration of multispectral sensors, *Remote Sens. Environ.* 22:11–37.

Smith, J. A., Tzeu, Lie Lin, and Ranson, K. J. (1980), The Lambertian assumption and Landsat data, *Photogramm. Eng. Remote Sens.* 46:1183–1189.

Staenz, K., Ahern, F. J., and Brown, R. J. (1981), The influence of illumination and viewing geometry on the reflectance factor of agricultural targets, in *Proc. 15th Symp. Remote Sens. Environ.*, ERIM, Ann Arbor, MI, pp. 867–882.

Tanré, D., Deroo, C., Duhaut, P., et al. (1986), Simulation of the satellite signal int he solar spectrum (5 S), Lab. d'Optique Atm., Lille, France, 147 pp.